J. Phys. B: At. Mol. Opt. Phys. 28 (1995) 435–444. Printed in the UK

# Three-body final-state momentum distributions for swift $H^+$ and $He^{2+}$ on He collisions

R Dörner†¶, V Mergel†, Liu Zhaoyuan‡, J Ullrich§, L Spielberger†, R E Olson‖ and H Schmidt-Böcking†

† Institut für Kernphysik, Universität Frankfurt, D60486 Frankfurt, Germany
‡ Lanzhou University, Lanzhou, People's Republic of China
§ GSI, D64291 Darmstadt, Germany
‖ Departement of Physics, University of Missouri-Rolla, Rolla, MI 65401, USA

Received 14 September 1994

**Abstract.** The transverse and longitudinal momentum distributions of $He^+$ ions produced by 0.25–1 MeV $u^{-1}$ $H^+$ and $He^{2+}$ impact have been measured using a precooled supersonic gas jet target (cold-target recoil ion-momentum spectroscopy—COLTRIMS). The transverse momentum of the recoil ions is mainly determined by the impact parameter. In the longitudinal direction the recoil ions are slightly backwardly directed. The width of the longitudinal momentum distribution is close to the electron momentum distribution in the initial state. This distribution gets much broader for larger transverse momentum transfer (i.e. smaller impact parameters). The experimental results are in good agreement with nCTMC calculations.

## 1. Introduction

The question of the momentum distribution in the three-body continuum final state is one of the most complex problems which arises for a singly ionizing atomic collision. The momenta of the emitted electron and of the projectile have been under study for many years. Whereas only a few experiments have been reported on the momentum distribution of the third particle, the recoiling target ion (Ullrich *et al* 1989, Dörner *et al* 1989, Ali *et al* 1992, Frohne 1993). The main reasons for this lack of data are the experimental difficulties that need to be overcome in order to measure this quantity.

In this work we present the transverse and longitudinal momentum distribution of $He^+$ ions created by 0.25–1 MeV proton and alpha particle impact. For these experiments the technique of cold-target recoil ion-momentum spectroscopy (COLTRIMS) (Dörner *et al* 1994, Mergel *et al* 1994, Ullrich *et al* 1994) which is based on a precooled supersonic gas jet target has been used. Due to the cold preparation of the target initial state, this method allows one to determine the momentum of the recoil ion to a precision of better than $\pm 0.13$ atomic units (au), a factor of 10 to 20 better than in former experiments on recoil ion transverse (see e.g. Ullrich *et al* 1989, Dörner *et al* 1989) and longitudinal (Ali *et al* 1992, Frohne *et al* 1993) momentum. Further, our technique allows one for the first time to measure the momenta of the ions in a fast ionizing collision with a resolution sufficient to resolve the small momentum transfers which are dominant at distant collisions and give the main contribution to the ionization cross section.

¶ E-mail address: Doerner@IKF.UNI-FRANKFURT.DE

0953-4075/95/030435+10$19.50  

## 2. Experiment

The experiment has been performed at the 2 MV van de Graff accelerator of the Institut für Kernphysik of the University of Frankfurt. The ion beam was collimated by two sets of adjustable slits placed about 0.3 m and 3.5 m upstreams of the interaction region. After the upstream slits an electrostatic deflector produced a chopped beam by applying a pulsed voltage of 50 V with a rise and fall time of below 5 ns and a repetition rate of about 8 kHz. The width of both sets of slits was about 0.2 × 0.2 mm, allowing for fast pulsing and delivering of a beam spot of the same size at the interaction point.

The recoil ion momenta expected in this experiment are of the order of a few atomic units (au) only, which is smaller than the initial target-atom momentum spread due to thermal motion at room temperature. Thus, the target gas has to be prepared to be extremely cold before the collision. This was achieved by using a precooled supersonic gas jet for the target (see figure 1). The He gas expanded through a 30 $\mu$m hole. The gas reservoir and the expansion hole were cooled to about 14 K by the cold finger of a cryo pump. About 10 mm from the gas outlet the coldest innermost part of the He jet passed through a skimmer of 0.3 mm diameter into the collision chamber. The gas jet left the collision chamber through a 1 cm diameter hole into a separately pumped beam dump. The He gas pressure was about 200 mb on the high pressure side of the expansion hole, $5 \times 10^{-4}$ mb in the skimmer chamber, and below $10^{-8}$ mb in the collision chamber. This gas jet intersects under 90° with the ion beam. The gas jet has a diameter of 1.1 mm at the intersection point and a target density of about $10^{11}$ particles/cm$^2$. The recoil ions created at the intersection point were accelerated by a homogeneous electric field of 0.3–1.5 V cm$^{-1}$ perpendicular to the gas jet and the ion beam. After passing a field-free drift region they are detected by a two-dimensional position-sensitive channel plate detector with a position resolution of about 0.2 mm. From the time of flight, measured in coincidence with the pulsed projectile beam, the recoil momentum in the direction of the field and the recoil ion charge state are obtained. The two other momentum components are extracted from the position of the recoil ion on the channel plate detector. Depending on the electric extraction field the maximum momentum acceptance of the detector is 4–8 au. The momentum resolution in the ion beam direction is restricted by the uncertainty in the starting point of the ion due to the diameter

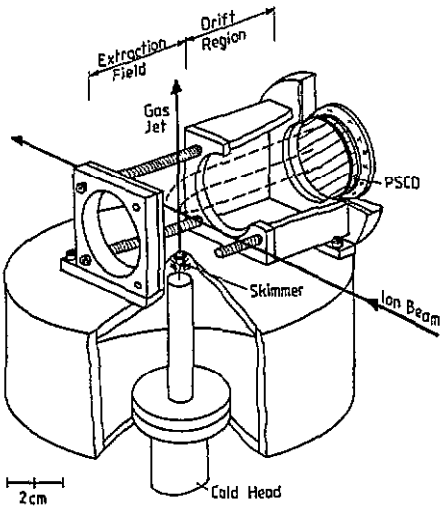


**Figure 1.** High-resolution recoil ion momentum spectrometer with precooled supersonic gas jet target.

of the gas jet to ±0.13–0.26 au (depending on the extraction voltage). In the two directions perpendicular to the ion beam the resolution is given by the internal temperature of the gas jet and is better than ±0.1 au.

Besides the preparation of a cold target, an exact determination of the zero point for the longitudinal momentum of the recoil ions is crucial for this experiment. This was done by measuring the longitudinal momenta for single capture reactions

$$He^{2+} + He \rightarrow He^{+} + He^{+} \tag{1}$$

$$He^{+} + He \rightarrow He + He^{+}. \tag{2}$$

For a capture reaction the longitudinal momentum of the recoiling ion $p_{\parallel \mathrm{rec}}$ can be deduced from energy and momentum conservation to be (Dörner *et al* 1991a, Mergel *et al* 1994)

$$p_{\parallel \mathrm{rec}} = \Delta E / v_{\mathrm{pro}} - n v_{\mathrm{pro}}/2 \tag{3}$$

where $\Delta E$ is the change in binding energy between the initial and final electronic states, $v_{\mathrm{pro}}$ is the projectile velocity, and $n$ is the number of captured electrons (atomic units are used throughout this paper). The $\Delta E/v_{\mathrm{pro}}$ term accounts for the fact that the projecitle loses or gains energy and the second term results from the change in momentum due to the mass transfer of the n electrons from the target to the projectile. Equation (3) shows that for a capture reaction discrete lines show up in the recoil longitudinal momentum distribution. From a capture reaction, therefore, one obtains directly the experimental resolution of the spectrometer. By calibrating to these known capture reactions an absolute calibration of the spectrometer can be made (Mergel *et al* 1994). Figure 2 shows the measured positions of the peak maxima for electron capture reactions (1) and (2) on the channel plate detector versus the calculated peak position given by (3). The full line is a least-squares fit through the data showing the linearity of the spectrometer and allows us to determine the zero position with an accuracy of better than ±0.05 au.

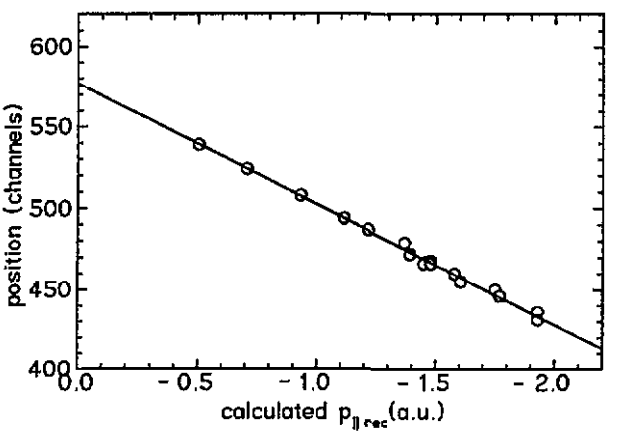


**Figure 2.** Calculated longitudinal momentum (from equation (3)) versus measured peak position on the recoil ion detector for reaction (1) at various impact energies. The full line shows a least-squares fit through the data, which was used for calibration of the spectrometer and determination of the position of $p_{\parallel} = 0$.

## 3. Results and discussion

The recoil ion momenta $p_{\parallel rec}$ and $p_{\perp rec}$ carry very different information on the collision process. From energy and momentum conservation it follows for an ionizing collision (Dörner *et al* 1991a):

$$p_{\parallel rec} = \frac{E_{bind} + E}{v_{pro}} - \sqrt{2E}\cos\vartheta_e = \frac{E_{bind} + E}{v_{pro}} - p_{\parallel}^{e} \tag{4}$$

$$p_{\perp rec} = m_{pro} v_{pro} \tan\vartheta_{pro} \sin\Phi_{pro\text{-}rec} + \sqrt{2E}\sin\vartheta_e \sin\Phi_{e\text{-}rec} \tag{5}$$

Both equations include one electron from projectile or target emitted to the continuum with continuum energy $E$ and a binding energy $E_{bind}$. $v_{pro}$ denotes the projectile velocity, $\vartheta_{pro}$ and $\vartheta_e$ the projectile polar scattering angle and the electron emission angle, $\Phi_{pro\text{-}rec}$ the azimuthal angle between projectile and recoil ions and $\Phi_{e\text{-}rec}$ the azimuthal angle between electron and recoil ion, respectively.

The data are compared to $n$-body classical trajectory Monte Carlo (nCTMC) calculations. A microcanonical distribution of the initial state of the He has been used with the centre of mass of the He target (nucleus and the two electrons) initially at rest. The classical equations of motions have been solved including the interactions between all particles besides the electron-electron interaction (Olson 1988).

### 3.1. Transverse momentum balance

Equation (5) shows that the transverse momentum of the recoil ion is, in general, the result of a complicated interplay between all the particles in the final state continuum. However, extensive studies of the projectile scattering angle dependence of the ionization cross section in $H^+$ on He collisions (Kamber *et al* 1988b, Kamber *et al* 1988a, Kristensen and Horsdal-Pedersen 1990, Salin 1989, Olson *et al* 1989) of the scattering angle dependence of the transverse recoil ion momentum (Dörner *et al* 1989, Dörner *et al* 1991b, Gensmantel *et al* 1992, Dörner *et al* 1993, Meng *et al* 1993, Fukuda *et al* 1991a, b) and of the scattering angle dependence of the projectile energy loss (Schiwietz *et al* 1994) lead to a detailed understanding of this transverse momentum balance in ionizing p–He collisions. This momentum exchange can be viewed from the perspective of all three particles in the final state. Each of these three tranverse momentum distributions highlights a different aspect of the ionization dynamics.

For the scattering of the projectile, i.e. viewed from the transverse momentum transfer to the projectile, three regions of momentum transfer can be recognized. At very small scattering angles (below 0.2 mrad) the recoil ion and electron are emitted opposite to each other (seen in the plane perpendicular to the ion beam), compensating their transverse momenta, while the projectile transverse momentum is small. At scattering angles around 0.55 mrad the transverse momentum exchange between projectile and emitted electron is dominant. 0.55 mrad is the maximum scattering angle for a proton being deflected by an electron at rest. This intermediate scattering angle regime is dominated by distant collisions with respect to the target nucleus, but close collisions with respect to the electron. This results in fast binary encounter electrons, i.e. large energy loss (Schiwietz *et al* 1994), but comparable small transverse momentum transfer to the recoil ion (Dörner *et al* 1989). Scattering angles much larger than the critical angle of 0.55 mrad can be reached only by scattering off the projectile by the target nucleus at a small impact parameter. In this regime of large scattering angles the electron transverse momentum is small compared with the recoil ion and projectile momenta (Dörner *et al* 1989, Gensmantel *et al* 1992).

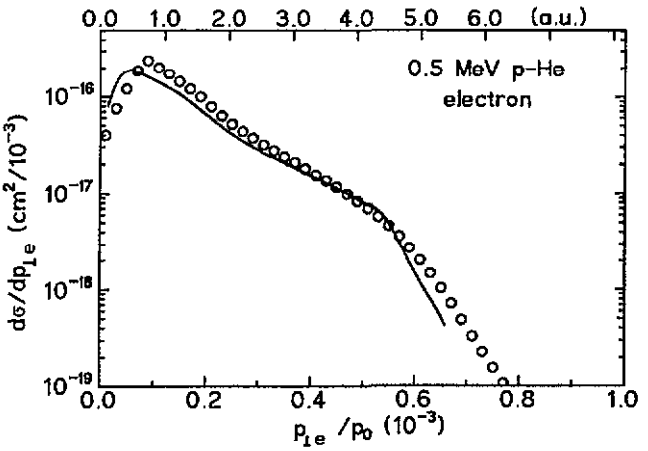


**Figure 3.** Transverse momentum distribution of emitted electrons for 0.5 MeV $H^+ + He \rightarrow p + He^+ + e^-$ experimental data from Rudd and co-workers (Rudd *et al* 1976) (for the transformation of the cross sections see text)—full curve: nCTMC. $p_0$ is the initial projectile momentum.

In a second perspective, now viewed from the transverse momentum transfer to the electron, the situation becomes simpler. The transverse momentum of the electron is dominated by the Rutherford scattering of the projectile at the electron. Since the electron is not at rest before the collision, this purely Rutherford scattering pattern is folded with the momentum distribution of the He ground state. To illustrate this fact we have calculated the transverse momentum distribution of the electron for 0.5 MeV p–He collisions from the double differential electron distribution $d^2\sigma/(d\vartheta_e dE)$ of (Rudd *et al* 1976) using

$$\frac{d\sigma}{dp_{\perp e}} = \int_0^{\pi} \frac{d^2\sigma}{d\vartheta_e\, dE} \frac{1}{\sin^2 \vartheta_e} p_{\perp e}\, d\vartheta_e . \tag{6}$$

The results are in good agreement with nCTMC calculations and show a decrease close to a Rutherford cross section with the cut-off at a transverse momentum transfer according to the critical scattering angle of 0.55 mrad (figure 3).

The third perspective, seen from the transverse momentum transfer to the recoil ion, is shown in figure 4. Similar to the case of the electron the recoil ion transverse momentum distribution measured in this work can be understood mainly through the Coulomb interaction between the projectile and the target nucleus. Thus the transverse momentum of the recoil ion reflects the internuclear impact parameter. In a crude approximation this cross section is therefore the Rutherford cross section multiplied by the ionization probability at the corresponding impact parameter. This simple picture is, however, complicated by two effects. First the final-state interaction between the emitted electron and the remaining ion has been neglected. Second and even more important, just like the electron, the target nucleus in an atom is not at rest, since only the complete three-body He atom is initially frozen. Thus, the nucleus has to compensate the momentum of the electrons at all times. For the remaining ion after an ionizing collision this would lead to a momentum distribution as given by the Compton profile, even in the hypothetical case that no momentum from the projectile is transfered to the nucleus in the collision.

The experimental resolution for the transverse momentum is better than 0.1 au. This corresponds to a scattering angle resolution for the projectile of about $10^{-5}$ rad which is a factor of 5–10 better than can be achieved by a measurement of the projectile. The

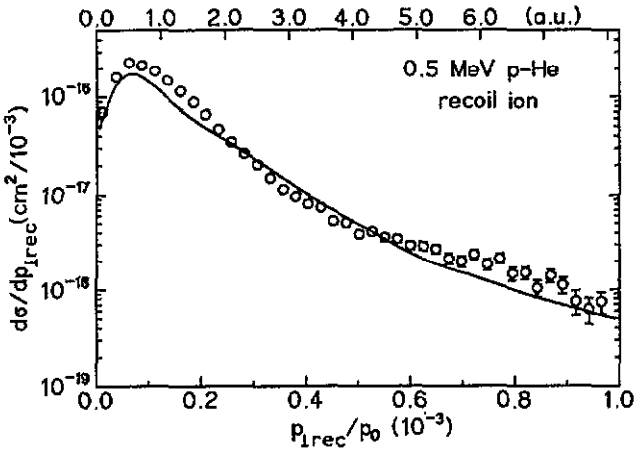


**Figure 4.** Transverse momentum distribution of recoil ions for 0.5 MeV $H^+ + He \rightarrow H^+ + He^+ + e^-$. Full curve: nCTMC. The units on the lower scale are equivalent to rad of the projectile scattering angle, $p_0$ is the initial projectile momentum.

exprimental results are in good agreement with the nCTMC calculation which incorporate all post-collision interactions as well as the effect of the moving nucleus in the initial state (figure 4).

### *3.2. Longitudinal momentum transfer*

The longitudinal momentum distributions of a singly-charged recoil ion created by various projectile energies and charges are shown in figure 5. Even though the projectile charge is varied from 1 to 2 and the impact velocity for proton impact is varied from 3.2 to 6.4 au we observe only minor changes in the longitudinal momentum distribution of the recoiling ions. The distribution is slightly backward-shifted and the shape is very similar to the Compton profile in the He atom which is shown for comparison in figure 5(*c*).

For the present collision system the projectile trajectory can be approximated by a straight line and the target nucleus does not move significantly in space during the collision. With these two assumptions the longitudinal momentum transfer due to the internuclear repulsion on the in- and outgoing half of the trajectory would cancel if the change in screening is neglected. This change in screening due to the emission of one electron can result in a net backward momentum transfer to the recoil ion. A more detailed analysis of this phenomenon is given by Horbatsch for the case of a highly charged ion colliding with Ne within the Vlasov model (Horbatsch 1994, Frohne *et al* 1993).

In most cases however, the emitted electron is slowly moving compared to the projectile. Therefore the main change in screening takes place after the projectile is already several atomic units away from the target leading to only a small backward momentum of the recoil ion. Moshammer *et al* (1994) report that in case of a highly charged projectile ($Ni^{28+}$) the situation changes due to the strong long-range projectile potential which pushes the recoil ions more strongly backward than observed in this work for low-$Z$ projectiles. In our case of fast, low-$Z$ projectiles impinging on He, the recoil ion longitudinal momentum distribution is quite similar to the He Compton profile (figure 5(*c*)). This indicates that very little momentum is tranferred from the projectile to the ion in the longitudinal direction. The ion momentum distribution is mainly given by its momentum in the initial state which

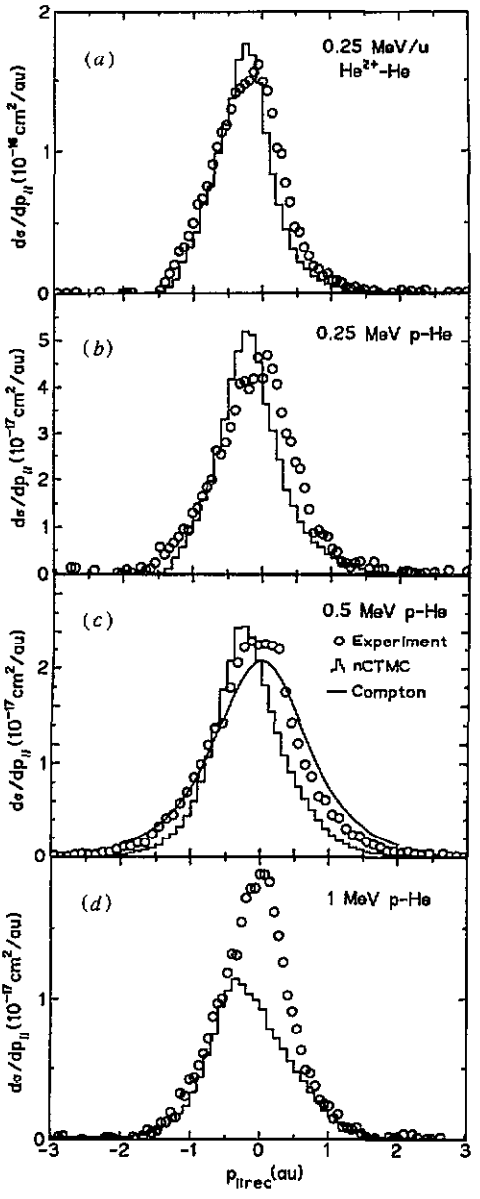


**Figure 5.** Longitudinal momentum distribution for $He^+$ recoil ions for various projectile charges and energies. Open circles: experiment, histogram nCTMC, full curve: ground-state momentum distribution (Compton profile) of He from Eisenberg (1970).

is set free in the collision since the electron is knocked out by the projectile.

The longitudinal momentum of the ions has been measured simultaneously to the transverse momentum. For the 0.5 MeV $H^+$ impact figure 6 shows the longitudinal momentum distribution for varying transverse momenta. A dramatic broadening in the momentum distribution is found in going to larger transverse momentum transfer, i.e. smaller impact parameters. Two effects may be responsible for the large longitudinal momenta at

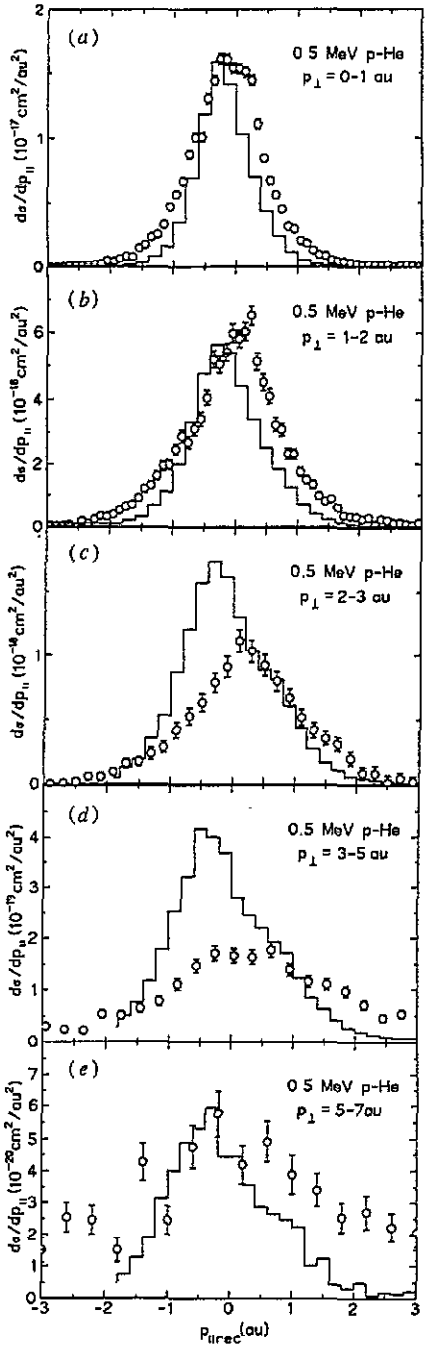


**Figure 6.** Longitudinal recoil ion momenum distribution for 0.5 MeV $H^+ + He \rightarrow H^+ + He^+ + e^-$, for various transverse momenta of the recoil ion.

small impact parameters. The high-momentum components of the electron wavefunction are located close to the nucleus. Thus removing such a fast electron will leave a hot ion

behind. In this respect the ion final state is a mirror of the fraction of the initial state which is picked out by the small impact parameter collision. This can be expected to become the dominant effect if the projectile and the emitted electron are fast. If this is not the case, then the electron, the target nucleus, and the projectile find enough time to exchange high momenta since for small impact parameter collisions they come together in a small volume.

We also emphasize that $p_{\parallel \mathrm{rec}}$ is directly connected to the electron energy and emission angle (equation (5)). For example, a binary encounter electron with $E = 2v_{\mathrm{pro}}^2 \cos \vartheta^2$ results for zero binding energy in $p_{\parallel \mathrm{rec}} = 0$. The data presented in figure 6 can therefore be used directly to check theoretical calculations for the impact parameter dependence of electron emission. Only very few (Jagutzki *et al* 1991, Schiwietz 1988, Skogvall and Schiwietz 1990, Skutlartz *et al* 1988) experiments have been reported so far where electron emission has been measured in coincidence with projectiles of defined impact parameter, since this is experimentally very difficult by conventional techniques.

In conclusion, we have measured the final-state momentum distribution of recoil ions created by swift $H^+$ and $He^{2+}$ impact. The transverse momentum results from the nuclear repulsion plus a part of the transverse momentum of the emitted electron. It is therefore partly related to the impact parameter of the collision. The longitudinal momentum is related to electron energy and angle. We find slightly backward emission of the recoil ion with a width of approximately the Compton profile. Only for small impact parameter collisions do we find much larger longitudinal momenta.

## Acknowledgments

The work was supported by DFG and BMFT. REO acknowledges support by the DOE—Office of Fusion Energy. We want to thank our friends and collegues C L Cocke, and M Schulz for helpful discussions and U Buck for helpful advise in the for construction of the gas target.

## References

Ali R, Frohne V, Cocke C L, Stöckli M and Raphaelian M L A 1992 *Phys. Rev. Lett.* **69** 2491–94

Dörner R, Ullrich J, Jagutzki O, Lencinas S, Gensmantel A and Schmidt-Böcking H 1991a *Electronic and Atomic Collisions, Invited Papers of the ICPEAC XVII* ed W R MacGillivray, I E McCarthy and M C Standage (Berlin: Hilger) p 351

Dörner R, Ullrich J, Jagutzki O, Lencinas S, Schmidt-Böcking H and Olson R E 1991b *Z. Phys.* D **21** 57

Dörner R, Ullrich J, Olson R E, Jagutzki O and Schmidt-Böcking H 1993 *Phys. Rev.* A **47** 3845

Dörner R, Ullrich J, Schmidt-Böcking H and Olson R E 1989 *Phys. Rev. Lett.* **63** 147

Dörner R *et al* 1994 *Phys. Rev. Lett.* **72** 3166

Eisenberg P 1970 *Phys. Rev.* A **2** 1678

Frohne V, Cheng S, Ali R, Raphaeilian M, Cocke C L and Olson R E 1993 *Phys. Rev. Lett.* **71** 696—9

Fukuda H, Shimamura I, Vegh L and Watanabe T 1991a *Phys. Rev.* A **44** 1565

Fukuda H, Watanabe T, Shimamura I and Vegh L 1991b *Nucl. Instrum. Meth.*

Gensmantel A, Ullrich J, Dörner R, Olson R E, Ullmann K, Forberich E, Lencinas S and Schmidt-Böcking H 1992 *Phys. Rev.* A **45** 4572–5

Horbatsch M 1994 *J. Phys. B: At. Mol. Opt. Phys.* **27** 2533

Jagutzki O, Koch R, Skutlartz A, Kelbch C and Schmidt-Böcking H 1991 *J. Phys. B: At. Mol. Opt. Phys.* **24**

Kamber E Y, Cocke C L, Cheng S, McGuire J H and Varghese S L 1988a *J. Phys. B: At. Mol. Phys.* **21** L455

Kamber E Y, Cocke C L, Cheng S and Varghese S L 1988b *Phys. Rev. Lett.* **60** 2026

Kristensen F G and Horsdal-Pedersen E 1990 *J. Phys. B: At. Mol. Opt. Phys.* **23** 4129

Meng C, Olson R E, Dörner R, Ullrich J and Schmidt-Böcking H 1993 *J. Phys. B: At. Mol. Opt. Phys.* **26** 3387

Mergel V *et al* 1994 *Phys. Rev. Lett.* accepted for publication

Moshammer R, Ullrich J, Unverzagt M, Schmidt V, Jardin P, Mann R, Dörner R, Mergel V and Schmidt-Böcking H 1994 *Phys. Rev. Lett.* accepted for publication

Olson R E 1988 *Electronic and Atomic Collisions* (Amsterdam: Elsevier) p 71

Olson R E, Ullrich J, Dörner R and Schmidt-Böcking H 1989 *Phys. Rev.* A **40** 2843

Rudd M E, Toburen L H and Stolterfoht N 1976 *Nucl. Data Tables* **18** 413

Salin A 1989 *J. Phys. B: At. Mol. Opt. Phys.* **22** 3901

Schiwietz G 1988 *Phys. Rev.* A **37** 370

Schiwietz G, Grande P P, Auth C, Winter H and Salin A 1994 *Phys. Rev. Lett.* **72** 2159

Skogvall B and Schiwietz G 1990 *Phys. Rev. Lett.* **65** 3265

Skutlartz A, Hagmann S and Schmidt-Böcking H 1988 *J. Phys. B: At. Mol. Phys.* **21** 3609

Ullrich J, Dörner R, Mergel V, Jagutzki O, Spielberger L and Schmidt-Böcking H 1994 *Commun. At. Mol. Phys.* accepted for publication

Ullrich J, Olson R E, Dörner R, Dangendorf V, Kelbch S, Berg H and Schmidt-Böcking H 1989 *J. Phys. B: At. Mol. Opt. Phys.* **22** 627